Desalination and Water Treatment
www.deswater.com

doi:10.5004/dwt.2019.23663

156 (2019) 136–147
July

Performance analysis of combined two stage desalination and cooling plant with different solar collectors

B. Anand[a,*], R. Shankar[a], T. Srinivas[b], S. Murugavelh[a]

[a]*CO_2 Research and Green Technologies Centre, VIT University, Vellore, India, Tel. (+91) 8870077224, email: anandgbea@gmail.com (B. Anand), gentlewise26@yahoo.com (R. Shankar), murugavelh.s@vit.ac.in (S. Murugavelh)*
[b]*Department of Mechanical Engineering, Dr. B.R. Ambedkar National Institute of Technology Jalandhar, India, email: srinivast@nitj.ac.in (T. Srinivas)*

Received 5 September 2018; Accepted 23 December 2018

ABSTRACT

An experimental investigation of a two stage desalination-cooling (TSDC) plant assisted by solar flat plate collectors (SFPC) is reported. From the experimental study the total power consumption, desalination yield, and cooling output were estimated. The potential of a concentrating photovoltaic thermal (CPVT)collector to achieve possible reduction in power consumption of the TSDC plant was explored for the same desalination and cooling output. A mathematical model of CPVT collector assisted TSDC plant was developed and validated. Both configurations are compared in terms of specific water production and plant energy utilisation factor (EUF). This study reveals that the highest specific water production and EUF of CPVT assisted plant are 0.12 kg/m^2-h and 0.23. For SFPC assisted plant the highest specific water production and EUF are 0.11 kg/m^2-h and 0.11 respectively. The use of CPVT collector in lieu of SFPC to operate the TSDC plant results in higher specific water production and energy utilisation factor. A lesser amount of electrical energy and collector area is sufficient to operate the TSDC plant assisted by CPVT collector compared to SFPC assisted plant for same output.

Keywords: Concentrated photovoltaic/thermal; Cooling; Desalination; Humidification; Power

1. Introduction

Increase in world population with accompanying increase in agricultural and industrial activity has resulted in excessive need of power, water and space cooling/heating. Process integration offers multiple benefits and it is a best way for decentralised power/energy production. Multiple outputs obtained from a single source of energy results in increased EUF of the plant. Multi stage flash (MSF), multi effect distillation (MED), and reverse osmosis (RO) are the currently used large scale centralized desalination plants where large amount desalinated water is produced and supplied to urban areas [1]. However, the decentralized plants for sustainable development are gaining significance attention in recent years. Solar energy integrated with humidification-dehumidification (HDH) desalination system is one of the best methods for small scale decentralised desalination due to its operational simplicity [2,3]. There are many kinds of solar technologies such as flat plate collector, evacuated tube collector, parabolic trough, dual purpose solar collector and solar pond integrated with HDH desalination system to supply required thermal energy [4–8]. It is reported that higher the solar radiation intensity greater is the productivity of distilled water [7].

Further, studies were also carried out on integration of air conditioning (A/C) and HDH water desalination assisted by solar energy. Such integration of cooling plant with HDH desalination results in increased desalination yield and cooling effect for air conditioning. The electrical power consumption, coefficient of performance (COP) of solar assisted A/C integrated HDH desalination system increases with increase in air temperature, air humidity and solar collector area. The highest water production and

*Corresponding author.

Presented at the InDA Conference 2018 (InDACON-2018), 20–21 April 2018, Tiruchirappalli, India

cooling load from the solar assisted A/C-HDH desalination system is 501 kg/d and 146.7 kWh respectively [9]. A parametrical and economic study on solar hybrid A/C and HDH desalination system under steady state operation reveals that the solar hybrid A/C-HDH system has higher water production, cooling capacity and COP compared with a basic air conditioning [10]. A novel polygeneration system with ejector refrigeration cycle and HDH desalination to simultaneously generate power, cooling, heating and distilled water is proposed by Sadeghi et al. [11]. Four different configurations of integrative A/C-HDH desalination system with evaporative cooler and heat recovery units were analysed at different locations [12]. A review on different refrigeration cycles (single effect absorption, double effect absorption, triple effect absorption and other types of vapor compression refrigeration cycle) concludes that at constant evaporator load of 3.516 kW, COP of VCR cycle is 56.89% higher than vapor absorption refrigeration cycle [13].

From the literatures studied, it is observed that the solar assisted integrated A/C and desalination system perform better than individually operated system. But these technologies require hot water for desalination and additional electrical energy to run auxiliary equipment of the integrated A/C and desalination system. In such cases, if PVT (Photovoltaic/thermal) collectors are used it would produce hot water for desalination and electricity to run the auxiliary equipment which will improve overall efficiency of the plant. Saouliotis et al. [14] presented an experimental and lifecycle assessment of PVT solar systems for domestic applications. An experimental investigation on a Peltier based hybrid PVT active solar still resulted in 30% higher efficiency than the conventional passive still [15]. A review on PVT integrated solar still concludes that PVT-solar stills are self-sustainable and PV cells can be fixed at the walls of solar still to reduce fixing cost of solar panel and to improve the efficiency of PV cells [16]. A PVT integrated HDH desalination system suitable for small scale water production in remote areas has resulted in 83.6% reduction in environmental impacts when compared with solar photovoltaic powered RO (reverse osmosis) system. The annual desalination and electricity generation are 833 L/m^2 of PV panel, 278 kWh/m^2 respectively [17]. Calise et al. [18] investigated a renewable polygeneration system for a small isolated community. The study found that the optimal ratio between solar field area and absorption chiller capacity is 5.9 m^2/kW. A feasibility study on CPVT driven liquid desiccant system for deep dehumidification achieved 55.6% of power savings compared with conventional technology [19]. The potential of PVT system for combined heating/cooling provision to households in the urban environment can be explored. The barriers for the market adoption of PVT technology are high initial cost and lack of advertising [20].

Thus, PVT collectors can be utilized as the source of electrical and thermal energy required for the integrated desalination and cooling process. The hybrid PVT systems are promising when the available area is restricted and when overall efficiency is of prime importance. Further the study reveals that the PVT systems are capable of reaching overall efficiency of 70% and it can cover more than 50–60% of cooling, heating needs of households [20].

The literature study indicates that more detailed study on solar assisted integrated cooling and desalination systems are still needed to be investigated in terms of energy savings, overall efficiency and collector area. Hence, this study aims to evaluate the potential and advantage of CPVT collector over conventional SFPC to operate the TSDC plant. A CPVT collector is a type of photovoltaic technology that simultaneously generates electricity and useful thermal energy form high intensity sunlight focused by lenses and curved mirrors. The MATLAB software tool was used for modelling and assessment. Initially experimental investigation of a SFPC operated TSDC plant was carried out. Based on the experimental analysis, the hot water and electrical power requirement of the desalination and cooling plant was estimated. Next, for the required amount of hot water and electrical power generation a mathematical model of CPVT collector was developed. The hot water temperature and electrical energy production in a CPVT system was controlled by controlling the mass flow rate of cooling water circulated back of the PV panel. The effect of mass flow rate of cooling water on system performance such as distilled water production, hot water temperature, PV efficiency and cooling output are investigated. Further, the performance of the proposed CPVT collector driven plant is compared with the SFPC driven plant focusing on specific water production and plant EUF for the purpose of evaluation of the objective of this work.

2. Methodology

The two configurations analyzed in this study are shown in Figs. 1 and 2. Each configuration consists of a TSDC system which gives advantage of increased desalination output and cooling yield. However, the mode of thermal energy supply to the TSDC system is different for the each configuration. In the first configuration (Fig. 1) the TSDC setup receives thermal energy from solar flat plate collectors, whereas in the second configuration (Fig. 2) utilizes thermal energy produced from a CPVT collector. The performance of the CPVT driven desalination and cooling plant is theoretically analyzed in terms of water outlet temperature from CPVT collector, desalination yield, PV efficiency and cooling yield then the results are compared with the experimental analysis of SFPC driven plant in terms of specific water production and plant EUF to analyze overall system performance.

2.1. Experimental setup of SFPC assisted two stage desalination and cooling plant

The experimental setup of solar flat plate collectors driven TSDC plant is show in Fig. 1. The setup comprises of solar flat plate collectors, air preheaters, humidifiers, dehumidifiers, pumps, blower and a chiller unit. The solar water heating system consists of 14 m^2 solar collectors connected in series. Saline water is indirectly heated in solar water heater by glycol water mixture which acts as a primary heat transfer fluid in solar flat plate collectors. The complete solar water heating system is placed at the rooftop to avoid shading and to capture maximum solar radiation. Hot water is supplied form solar water heater to air preheaters, humidifiers of first and second stage desalination in parallel pipe connections. Air is supplied from a blower to the

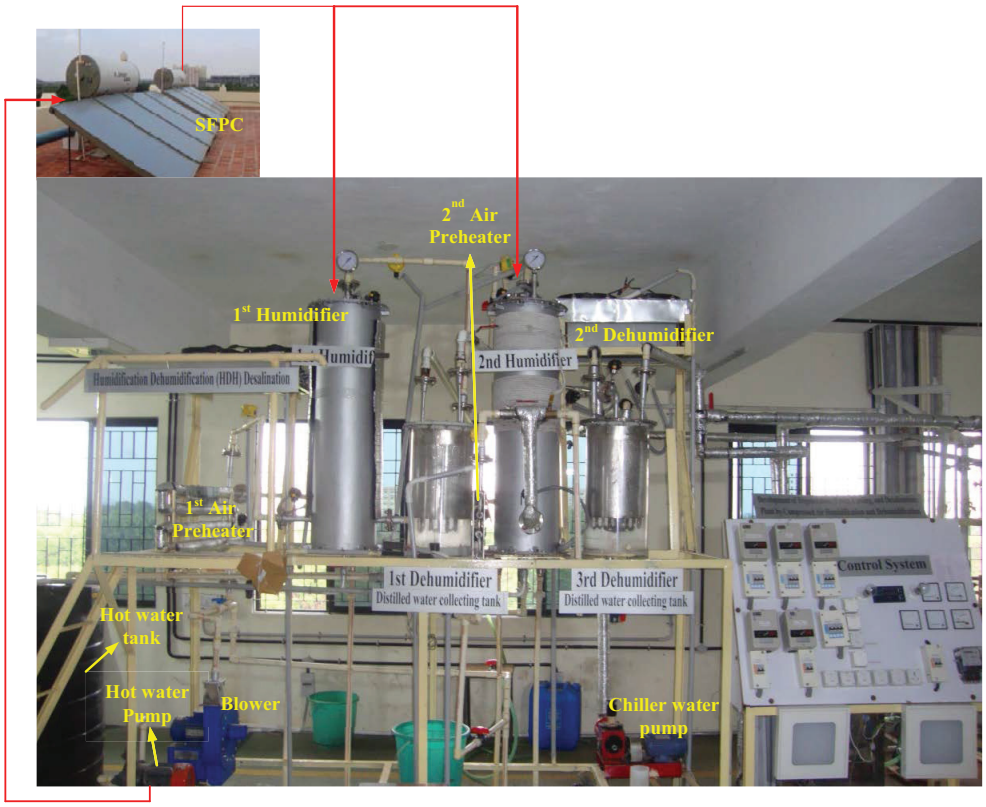

Fig. 1. Experimental setup of solar flat plate collectors assisted two stage humidification-dehumidification desalination and cooling plant.

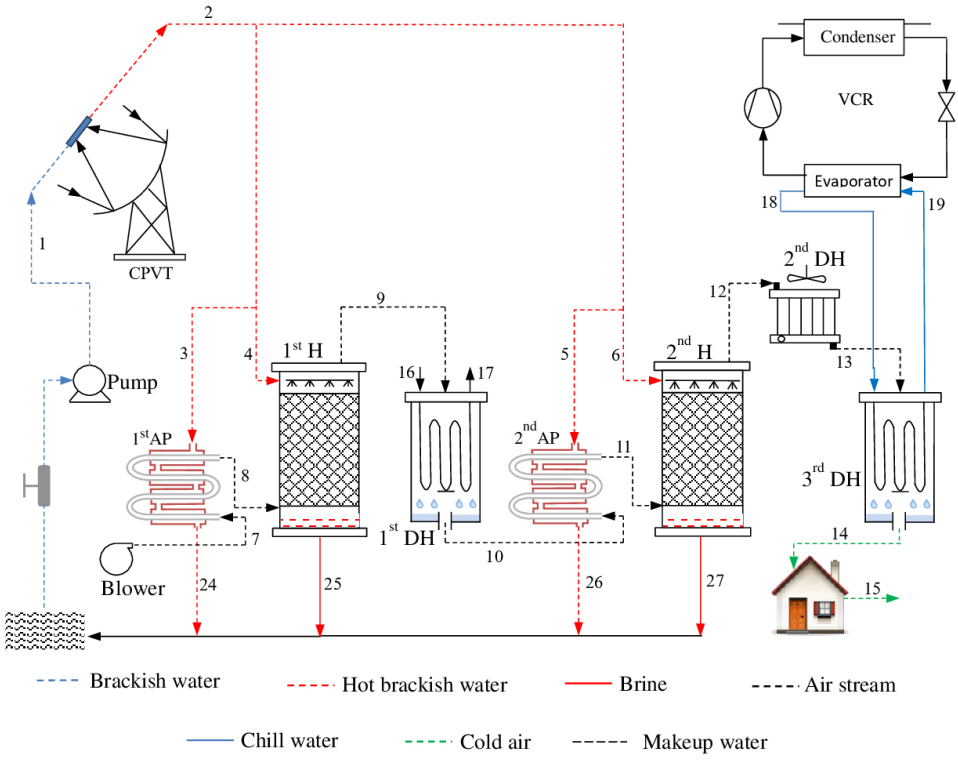

Fig. 2. Process flow diagram of concentrated photovoltaic/thermal driven two stage humidification-dehumidification desalination and cooling plant.

desalination plant. The blower used in this work is manufactured by CLEANTEK and the model is CB-0.5. It has the maximum discharge capacity of 500 m^3/h (642 kg/h). Air preheaters are concentric tube heat exchanger (made of SS 304 material) consists of 4 tubes of 12 mm diameter and each 1000 mm long. The tubes are enclosed by an outer tube of diameter 25 mm. The air flows in the outer pipe of the heat exchanger (annulus) and hot water flows in the tube side. After preheating of air from the first air preheater, hot air is sent to the first humidifier. The humidifiers are vertical cylinders (SS 304 material) of 1500 mm height and 300 mm of diameter. The humidifiers are filled with honeycomb structured plastic packing. Hot water is sprayed at top of the humidifiers, collected at bottom and drained to hot water tank for recirculation. After heating and humidification, the hot humid air is sent to the first dehumidifier where the water vapor in the hot humid air is condensed by circulating normal cooling water. Later the air from the first stage desalination is again preheated and humidified in the 2nd air preheater and 2nd humidifier of second stage desalination. The second stage desalination has two dehumidifiers i.e. the 2nd dehumidifier (air cooled) and third dehumidifier (chill water cooled). The first and third dehumidifiers are shell and tube heat exchanger consisting of tubes (25 tubes) and acrylic shell to visualize the dehumidification process. The tubes of first and third dehumidifiers are made of SS 304 material with each 12 mm of diameter and 500 mm of length. The acrylic shells are 300 mm of diameter and 700 mm of height. In the first and third dehumidifier, humid air flows in shell side, water flows in the tube side. A 0.5 hp compressor operated chiller unit supplies chilled water to third dehumidifier. The 2nd dehumidifier reduces load on 3rd dehumidifier. It is a cross flow plate fin type tube compact heat exchanger with copper tubes (50 tubes each 500 mm long) and aluminum fins. The 2nd dehumidifier reduces chilled water demand. The 2nd and 3rd dehumidifiers are connected in series and desalination occurring in 2nd dehumidifier is pooled up and collected in the 3rd dehumidifier. The actual pressure drop during experimentation was around 0.50 bar. The air pressure was measured using bourdon pressure gauge in the first humidifier and in the second humidifier. In order to avoid the large pressure drop, only 25% of the air supplied to the 2nd dehumidifier. The complete desalination and cooling setup is elevated to 1.5 m using a stand for easy collection of water and chill air. Electrical connections are given and for easy access all the switches are named, arranged on a control board which is placed in front of the chiller unit.

The assay was carried out in the geographical location of Vellore, India having 12.91°N latitude, 79.13°E longitude. The experimentation was conducted for different sunshine hours. The global radiation varied from 750 W/m^2 to 1000 W/m^2 throughout the sun shine hours. The daily average global radiation is 960 W/m^2. The hot water flow rates to the first and second humidifiers are same and it is calculated as 100 kg/h. The air flow rate to the desalination plant is calculated to be 20 kg/h. The other working parameters such as circulating water flow rate to the first dehumidifier, chilled water flow rate to the third dehumidifier are fixed in all sunshine hours. Experimentation is started after closing the air vent in the solar water heater to form a closed loop. In order to stop the humid air leak and to attain proper desalination, initially all the water pumps are switched on then gradually valves are opened to let the water flow into humidifiers and into dehumidifiers. Then the air is gradually supplied to the desalination plant and the plant is allowed to reach steady state operation. The distilled water produced in the first and second stage of desalination is collected in a column at the bottom of the dehumidifiers. Table 1 shows different measuring instruments used while doing experimentation with its accuracy level.

The sizing of the suitable CPVT system demands the best operating conditions to meet capacity of the desalination and cooling plant. The concentrated photovoltaic/thermal system is sized and simulated in such a way that it should be able to supply required hot water to the TSDC plant. Based on the experimental results, the CPVT system is sized and designed to supply same hot water temperature produced by the solar flat collectors of the TSDC plant for easy comparison. Increasing cooling water circulation rate in CPVT system reduces hot water temperature but reducing the flow rate results in lower electrical power generation. So the cooling water flow rate to the CPVT system is maintained in such a way to achieve required hot water temperature as well as electrical power.

2.2. Theoretical model of CPVT assisted two stage desalination and cooling

A schematic diagram of the proposed CPVT driven TSDC system is shown in Fig. 2. The system consists of a point focus parabolic dish collector, air preheater, humidifier, dehumidifier, chiller unit, pump, blower and a triple junction (InGalnP/InGaAs/Ge) solar photovoltaic /thermal panel placed on the receiver of the parabolic dish collector. The concentration ratio and aperture area of the CPVT system are 200 and 12 m^2. The active module size is 0.25 × 0.20 m. The PVT panel is cooled by circulating saline water (1) through the pipes attached to the back of the PVT panel. The

Table 1
Technical specifications of measuring instruments

Parameter	Measuring instrument	Model	Range	Accuracy
Air velocity	Digital Anemometer	AVM-03	0–45 m/s	±0.2 m/s
Fluid flow rate	Rotameter	RSA-3240	0–400 LPH	±0.5 LPH
Relative humidity	Humidity sensor	TRH-304	0–100% RH	±2 %RH
Solar radiation	Pyranometer	GEO-SR11	0–2000 W/m^2	±2 W/m^2
Temperature	Thermocouple	K-type	0–200 °C	±0.5 °C

hot saline water leaving (2) the collector is supplied to the TSDC plant. A blower located at the inlet of airpreheater-1 (1st AP) supplies air at atmospheric condition (7) to the two stage desalination system with an air flow rate of 20 kg/h. The average temperature and relative humidity of air at the inlet of desalination plant are 32 °C and 65% respectively. The air entering the humidifier (8) is preheated in first air preheater by hot saline water (3) supplied from the CPVT collector. Since the temperature of saline water (4) entering humidifier-1 (1st H) is greater than the preheated air, results in heating and humidification in the humidifier-1. After latent heat transfer takes place in the humidifier 1, the hot humid air (9) which has high relative humidity and specific humidity is sent to the dehumidifier-1 (1st DH). The hot humid air is cooled below its dew point temperature by heat transfer to the circulating water (16-17) supplied from an overhead storage tank. The fresh distilled water is collected at the bottom of the dehumidifier-1. The air (10) exiting from the dehumidifier -1 undergoes same process in the second stage desalination. In the second stage desalination the hot humid air (12) coming from humidifier-2 (2nd H) is initially dehumidified (13) by air cooled dehumidifier (2nd DH) to reduce cooling load of the chiller unit. Later for centralized air conditioning it is again dehumidified in the dehumidifier-3 (3rd DH) which receives chill water (18) from the vapor compression refrigeration (VCR) unit. The air (14) exiting from the dehumidifier-3 is at low temperature suitable for air conditioning. The identified operating parameters are hot water temperature supplied to the humidifiers and chilled water temperature supplied to the 3rd dehumidifier.

Based on the experimentation the following design and operating variables are assumed for the theoretical evaluation of CPVT driven desalination and cooling plant.

- Air flow rate at the inlet of desalination plant is 20 kg/h.
- Air preheater effectiveness is 50%.
- Humidifier efficiency is 30%.
- Since the overhead storage tank capacity is 5000 L, the changes in the water temperature are negligible. So the temperature and mass flow rate of cooling water enters the first dehumidifier are fixed as 30 °C and 300 kg/h.
- Mass flow rate of chill water enters the third dehumidifier is 125 kg/h.
- The total electrical energy consumption (including blower, hot water pump, chill water pump and compressor for VCR is 1.8 kWh.

3. Mathematical modeling

A mathematical model of CPVT driven HDH desalination system is developed. The first part of it is modeling of concentrated photovoltaic thermal system and the second is two stage HDH desalination and cooling system.

3.1. Modelling of CPV/T system

The CPVT system is developed based on the hot water and electrical power requirement of the desalination and cooling system which is observed from the experimental readings. The hot water temperature and electrical energy production in a CPVT system can be controlled by controlling the mass flow rate of the cooling water circulated back of the PV panel. Further for mathematical modeling, Eqs. (1)–(7) are adapted from [21–24].

The simple energy balance of the receiver is given in Eq. (1)

$$Q_{total} = Q_u + Q_l + P_e \tag{1}$$

where Q_l is the heat loss from the front and back side of the receiver, P_e is the electrical power produced from the PV module and Q_u is the useful energy from the receiver. Since front part of the PV module is exposed to concentrated solar radiation, heat loss from the front side (Q_f) includes both convective and radiative heat transfer. The convective and radiative heat loss from the front side is

$$Q_f = h_f A_f \left(T_c - T_a\right) + \varepsilon A_f \sigma \left(T_c{}^4 - 0.5 T_a{}^4\right) \tag{2}$$

where ε is emissivity of the cell that is equal to 0.85. After the front loss, the remaining thermal energy is transferred through the substrate to the cooling medium.

The back surface of the receiver is also exposed to the atmosphere. The convective and radiative heat loss from the back side of the receiver (Q_b) to the atmosphere is

$$Q_b = h_b A_b \left(T_b - T_a\right) + \varepsilon_b A_b \sigma \left(T_b{}^4 - T_a{}^4\right) \tag{3}$$

To calculate the electrical power it is necessary to consider PV efficiency (η_{pv}) and optical efficiency (η_{opt}). The value obtained from this has to be reduced by considering parasitic power (Q_{par}) consumption and inverter efficiency (η_{inv}). The parasitic power consumption is considered as 0.023 times of total radiation [22]. The net electrical power (P_e) the CPVT system can be calculated using Eq. (4).

$$P_e = \left(I_{bm} \cdot A_{ap} \cdot \eta_{opt} \cdot \eta_{pv}\right) \eta_{inv} - Q_{par} \tag{4}$$

where PV efficiency is product of cell efficiency (η_c) and module efficiency (η_{mod}) . The cell efficiency varies with cell temperature and concentration ratio (C) of the solar collector. Hence, considering module efficiency as 0.6, the cell efficiency is calculated as

$$\eta_c = 0.298 + 0.0142 \cdot \ln(C) + \left(-0.000715 + 0.0000697 \cdot \ln(C)\right)\left(T_c - 25°\text{C}\right) \tag{5}$$

where the cell temperature (T_c) is the function of ambient temperature, wind speed and direct normal irradiation and it is given in [23].

Finally the total useful thermal energy (Q_u) available is

$$Q_u = m_{bw} C_{p-bw} \left(T_2 - T_1\right) = h_c A_c \cdot \Delta T_{lm} \tag{6}$$

where h_c and A_c are convective heat transfer coefficient and heat transfer area respectively. Further details on calculation of convective heat transfer coefficient and log mean temperature between the receiver and the coolant (ΔT_{lm}) are referred from [24]. Note that thermal efficiency (η_{th}) of the CPV/T system is the ratio of total thermal energy used to the total thermal energy available which

$$\eta_{th} = \frac{m_{bw} C_{p-bw} \left(T_2 - T_1\right)}{I_{bm} A_{ap}} \tag{7}$$

3.2. Modelling of two stage desalination and cooling plant

The modelling of two stage desalination and cooling system is presented in this section. The mathematical expressions Eqs. (8)–(13) for the modelling of two stage desalination and cooling plant was referred from [25].

The air preheater exit air temperature is determined from its effectiveness as

$$T_8 = T_7 + \varepsilon_{APH}\left(T_4 - T_7\right) \tag{8}$$

Mass and energy balance of first humidifier and first de-humidifier is given by Eqs. (9), (10).

$$m_{air}(h_8 - h_9) = m_w h_4 - m_{br} h_{20} \tag{9}$$

$$m_{air}(h_{10} - h_9) = m_{dw} h_{dw} - m_{cw} C_{p-cw}(T_{17} - T_{16}) \tag{10}$$

The maximum and required water to air flow ratio of the humidifiers are calculated using the Merkel method [26].

$$\frac{h_4 - h_{20}}{h_s - h_{air}} = eH\left[\frac{m_w}{m_a}\right]^{-n} \tag{11}$$

where H is height of the packing material. Since, corrugated plastic sheets are used as packing material the values of constants e, n are 0.691 and 0.69 respectively. The graphical outputs of this equation are show in Figs. 3 and 4.

Similar to the first stage desalination, the energy balance equations, maximum and required water to air flow ratio for second stage desalination is carried out. The total desalination output from first and second stage desalination is

$$m_{dw} = m_{air}\left(w_9 - w_{10}\right) + m_{air}\left(w_{13} - w_{14}\right) \tag{12}$$

The cooling output from the third dehumidifier is evaluated by means of coefficient of performance as follows

$$COP = \frac{Q_c}{W_{comp}} = \frac{m_{air}\left(h_{ambient} - h_{14}\right)}{m_{ref}\left(h_{21} - h_{20}\right)} \tag{13}$$

where W_{comp} represents the electric power consumed by the compressor to operate the vapor compression unit.

The mass and energy balance for the components of VCR unit are as follows Eqs. (14)–(16) [27]

Heat rejected by the condenser (Q_{cond}) of VCR unit to the ambient is

$$Q_{cond} = m_{ref}\left(h_{21} - h_{22}\right) = m_{coolent}\left(h_{28} - h_{29}\right) \tag{14}$$

Since it is an is enthalpic expansion in capillary tube, the energy balance for the expansion process in capillary tube is

$$h_{22} = h_{23} \tag{15}$$

The required load of the evaporator is calculated by

$$Q_{evap} = m_{water} C_{p-water}\left(T_{19} - T_{18}\right) = m_{ref}\left(h_{23} - h_{20}\right) \tag{16}$$

where m_{ref} is mass flow rate of refrigerant (kg/s), $C_{p\text{-}water}$ is specific heat of water (kJ/kg °C).

The overall performance of two stage HDH desalination is evaluated in terms of specific water production. Further to consider electrical power generated by the CPVT collector and cooling effect (Q_c) from TSDC system, both plants (Figs. 1 and 2) are evaluated by plant EUF.

$$EUF_{plant} = \frac{Q_{dw} + P_e + Q_c}{A_a I_{bm} + P_{in}} \tag{17}$$

where Q_{dw} is equivalent heat of vaporization of distilled water, P_{in} is power supplied to the plant and P_e is power output from the plant.

To verify the mathematical model presented in this study, the simulated values are compared with experimental values and deviations are given in Table 2 and Table 3. The desalination yield for various hot water temperatures from 54.70 °C to 48.60 °C was observed experimentally for the fixed air flow rate of 20 kg/h. It shows that the maximum deviation from the experimental results is 9.79%. Table 3 shows the effect of cell temperature on conversion efficiency under different concentration ratio. The simulated values for different cell temperature under different concentration ratio are compared with experimental values [28]. The maximum deviation of cell efficiency from experimental value is 4.90%.

4. Results and discussion

The data collected in this study was obtained from two different solar collectors driven desalination and cooling plants such as solar flat plate collectors driven plant and solar concentrated photovoltaic/thermal driven plant. The similarity between these two systems is that both of the plants use TSDC system which gives an added advantage of increased desalination yield along with cold air for air conditioning. However, it consumes additional electricity for the production of cold water. In addition to this, electricity is also consumed by different auxiliary equipments such as pump, blower etc. Hence, Integration of suitable solar collector to the present desalination and cooling system will increase the overall performance by proving electricity and thermal energy required. In this study, the performance of the CPVT driven desalination and cooling plant is theoretically analyzed to investigate the merits of CPVT

Table 2
Validation of simulation with experimental results of desalination yield from two stage desalination and cooling plant

Hot water temperature, (°C)	Desalination, LPH		Deviation (%)
	Simulation	Experimental	
54.70	1.29	1.43	9.79
53.18	1.23	1.34	8.20
51.83	1.20	1.28	6.25
50.63	1.16	1.12	–6
49.56	1.12	1	–12

Table 3
Model validation: Cell efficiency under different concentration ratio and cell temperature

Cell temperature, (°C)	Conversion efficiency, (%) at 1000 W/m^2								
	C_r = 1			C_r = 17			C_r = 200		
	Present study	Nishioka et al. [28]	Deviation (%)	Present study	Nishioka et al. [28]	Deviation (%)	Present study	Nishioka et al. [28]	Deviation (%)
20	30.16	30	0.53	34.08	34.9	–2.40	37.50	37	1.33
40	28.73	28	2.54	33.05	34	–2.87	36.81	36.5	0.84
60	27.30	27.5	–0.73	32.01	33	–3.09	36.11	36	0.30
80	25.87	26	–0.50	30.98	32.5	–4.90	35.42	35.5	–0.22
100	24.44	25	–2.29	29.94	32	–0.68	34.73	35	–0.78

driven plant over the conventional SFPC driven plant. The operational parameters are outlet temperature from CPVT collector and mass flow rate of cooling water in to the CPVT collector. The focused outputs are desalination yield, PV efficiency and cooling yield. The theoretical results are compared with the experimental analysis of solar flat plat collectors driven plant in terms of specific water production and plant EUF for analyzing overall system performance. The comparison study is made between solar flat plate collector and CPVT collector as the output from both cases (flat plate collectors and CPVT collector) is hot water. The additional advantage of CPVT collector is that it produces electricity which can be used in auxiliary components.

Fig. 3 shows the humidifier simulation result to find out the maximum hot water to air mass ratio. The average temperature and relative humidity of the air at inlet of the desalination plant are considered as 32 °C and 55%. The maximum limit and required water to air mass ratio for the given height of the humidifier is calculated by assuming the hot water inlet temperature to the humidifier as 60 °C [25]. The hot water to air mass ratio has been increased from 1, with an interval of 0.5 to find out the maximum limit of mass ratio. The saturation line crosses the humidification line at the mass ratio of 9. The required mass ratio can be determined from the intersection of Merkel integral and packing function curve as shown in Fig. 4. Since the two functions are equal at a mass ratio of 5, the hot water flow rate at the inlet of humidifier can be calculated from air flow rate and required temperature difference. From this 100 kg/h of hot water is required for air flow rate of 20 kg/h.

Fig. 5 shows the effect of mass flow rate on cell temperature. It is observed that higher the mass flow rates lower is the cell temperature which results in high conversion efficiency. At 300 kg/h of water flow rate through PV panel, cell temperature was around 54.5 °C. As the flow rate reaches 400 kg/h the cell temperature drops to 48.3 °C. But increasing the water flow rate also reduces water temperature leaving the PV panel. The required hot water temperature and cell temperature can be controlled by controlling the water flow rate through the PV panel.

Fig. 6 depicts the role of mass flow rate on PV efficiency and improved efficiency. Here, improved efficiency is the change in efficiency of PV panel when water is circulated through the CPVT system compared to the efficiency of PV panel when there is no water circulated at same solar radiation level. Increasing the flow rate slightly increases

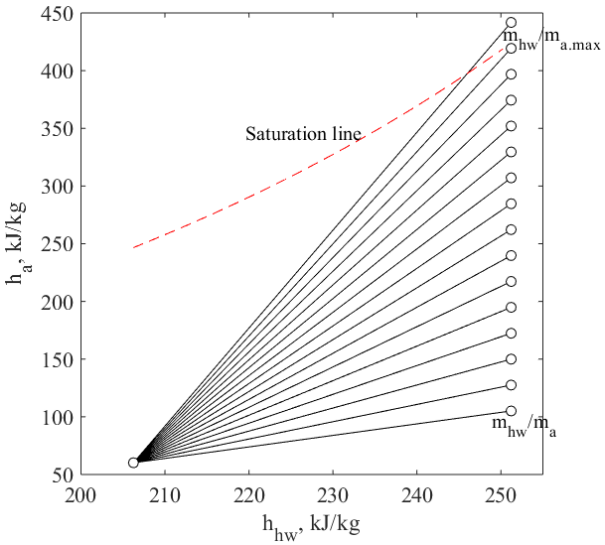

Fig. 3. Humidifier simulation to find maximum water to air mass ratio.

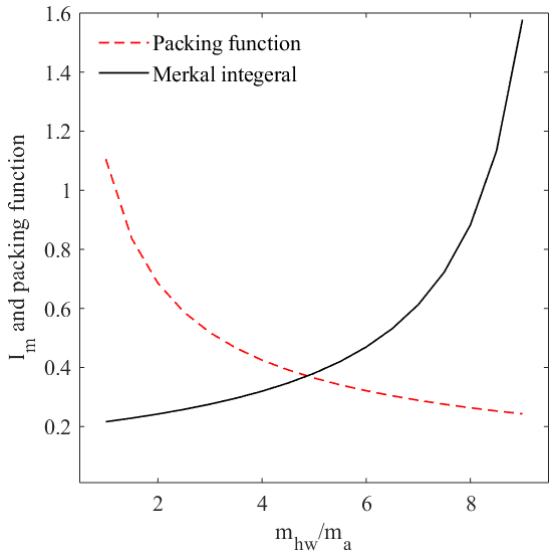

Fig. 4. Humidifier simulation to find out required water to air mass ratio.

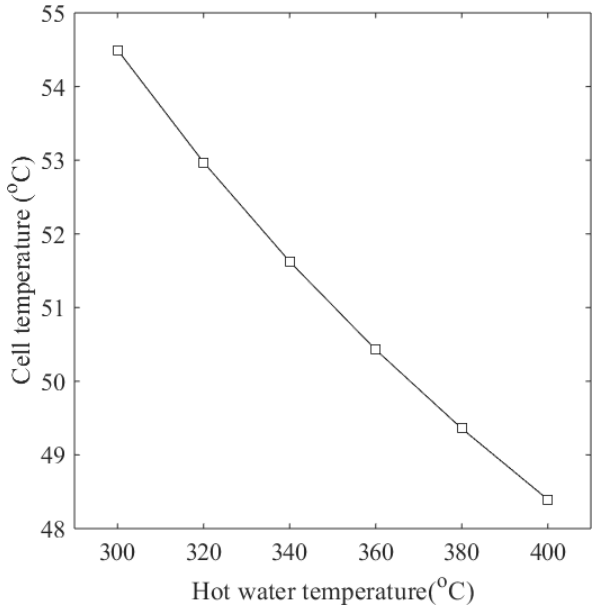

Fig. 5. Effect of water flow rate through CPVT collector on cell temperature.

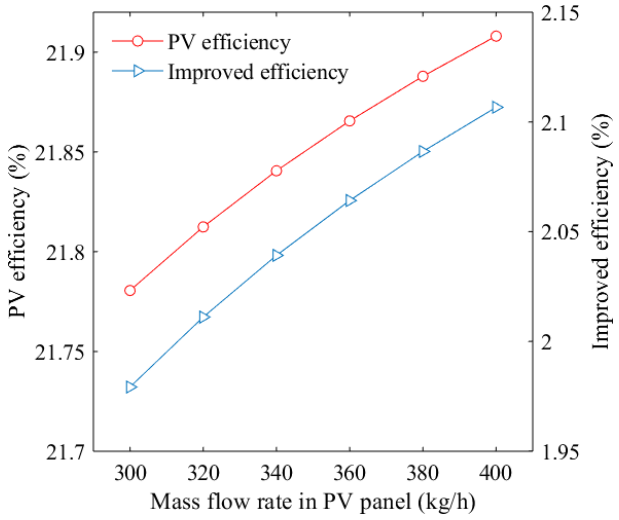

Fig. 6. Effect of water flow rate through CPVT collector on PV efficiency and improved efficiency.

PV efficiency. At 300 kg/h the efficiency of PV panel is 21.78% which is further increased to 21.91% at 400 kg/h. The change in PV efficiency while increasing the flow rate from 300 kg/h to 400 kg/h is found to be very small (0.13%). Meanwhile improved efficiency is found be slightly higher (2.14%) at 400 kg/h. The highest PV efficiency and improved efficiency is around 21.91% and 2.14% at 400 kg/h.

Fig. 7 shows the effect of mass flow rate on the electrical power production and improved electrical power. Here, improved electrical power is the change in electrical power production from PV panel when water is circulated through the CPVT system compared to the electrical power production from PV panel when there is no water circulated at same solar radiation level. Increasing the

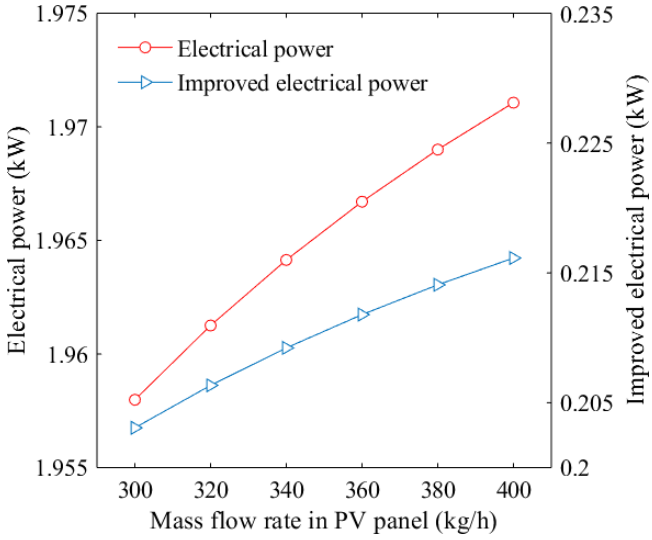

Fig. 7. Effect of water flow rate through CPVT collector on electrical power and improved electrical power.

flow rate to 400 kg/h resulted in highest PV efficiency, which increased the electrical power production. At mass flow rate of 300 kg/h, electrical power is around 1.957 kW which further increased to 1.972 kW at 400 kg/h of mass flow rate. This is due to rise in PV efficiency as the mass flow rate increases. But the change in electrical power generation is very small (0.015 kW) when mass flow rate is increased from 300 kg/h to 400 kg/h. Meanwhile, compared to PV panel without cooling, PV panel with cooling maximized the electrical energy production by 0.217 kW at 400 kg/h of mass flow rate. It is clear that for the fixed solar radiation level, presence of water cooling through the CPVT panel plays major role in increasing electrical power generation by increasing the PV efficiency. Meanwhile changes in mass flow rate have very small influence on power generation and higher the mass flow rate results in reduced water outlet temperature. This reduces the efficiency of humidification process in humidifier and results in reduced distilled water production.

Fig. 8 shows the effect of water flow rate through CPVT collector on water outlet temperature and distilled water production. The hot water temperature and distilled water production decreases as the water flow rate through the CPVT collector increased from 300 kg/h to 400 kg/h. Increasing the water flow rate decreased the inlet water temperature to the humidifiers, which decreased the efficiency of latent heat and mass transfer process takes place in the humidifiers. Hence, the distilled water production in both the first stage as well as in the second stage decreases as the mass flow rate increases in CPVT collector. Compared to the first stage desalination, second stage gives higher distilled water production as the chilled water from the chiller unit is used in the third dehumidifier. This results in maximum desalination yield with additional energy input for production of chilled water and its pumping. The highest distilled water production from the combined first and second stage is around 1.3 L/h for the hot water temperature of 54.70 °C.

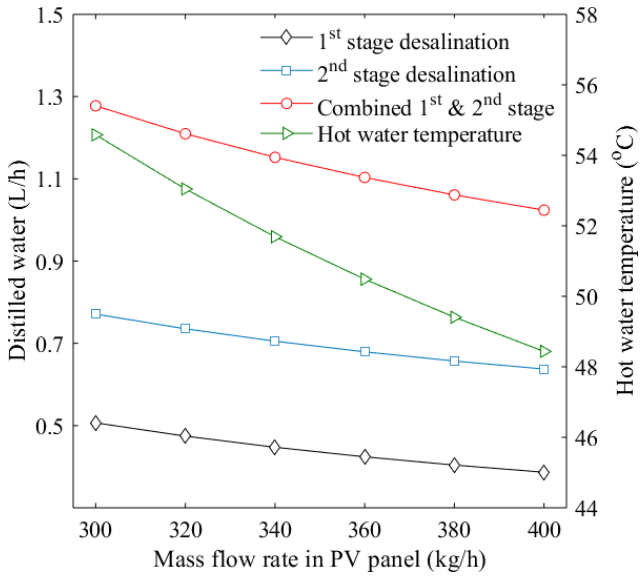

Fig. 8. Effect of water flow rate through CPVT collector on water outlet temperature and distilled water production.

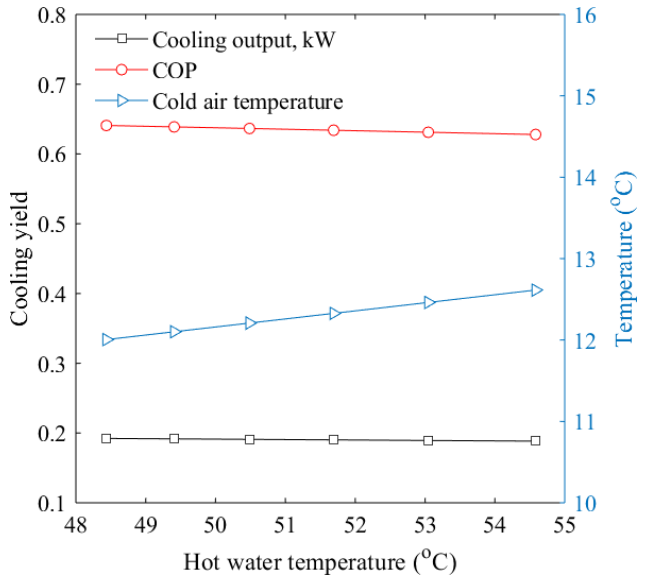

Fig. 9. Role of hot water temperature on cooling yield and cold air temperature of CPVT driven plant at 10 °C chilled water temperature to 3rd dehumidifier.

Figs. 9–11 depicts the role of hot water inlet temperature to the humidifiers and chilled water temperature to the dehumidifiers. The third dehumidifier chilled water temperature is varied as 10 °C, 15 °C, 20 °C and the cooling output was studied. In all the three cases, increasing hot water temperature increases air temperature that comes out of the third dehumidifier. This result in reduced cooling output and COP. Meanwhile, the temperature of air coming out of the 3rd dehumidifier drops and cooling yield increases as the chilled water temperature drops from 20 °C to 10 °C. But, during experimentation it was difficult to maintain 10 °C in chilled water storage tank as the chilled water leaving the 3rd dehumidifier recirculated to chilled water storage tank. During experimentation the chilled water temperature in the storage tank is measured as 15 °C.

Fig. 12 depicts the role of hot water temperature on cooling yield and cold air temperature of SFPC driven plant at 15 °C chilled water temperature to 3rd dehumidifier. The cold air temperature at the exit of the 3rd dehumidfier rises from 16.8 °C to 18.53 °C as the hot water temperature rises from 48.60 °C to 54.70 °C. Both the cooling output and COP drops as the hot water temperature rises. A maximum COP and cooling output of 0.5159 and 0.192 kW was achieved at hot water temperature of 54.70 °C.

The effects of cooling water flow rate through the CPVT collector on hot water temperature, desalination output, PV efficiency, electrical power production, and cooling output has been discussed in the above section. Further the desalination yiled from the CPVT driven plant and solar flat plate collectors driven plant is also compared in terms of specific water production. Apart from desalination and cooling, CPVT operated plant also produces electrical power. Therefore the total benefit from the plant is evaluated and compared in terms of energy utlization factor of plant.

As shown in Fig. 13, the specific water production from the CPVT driven plant is compared with the experimental values of solar flat plate collectors operated TSDC plant.

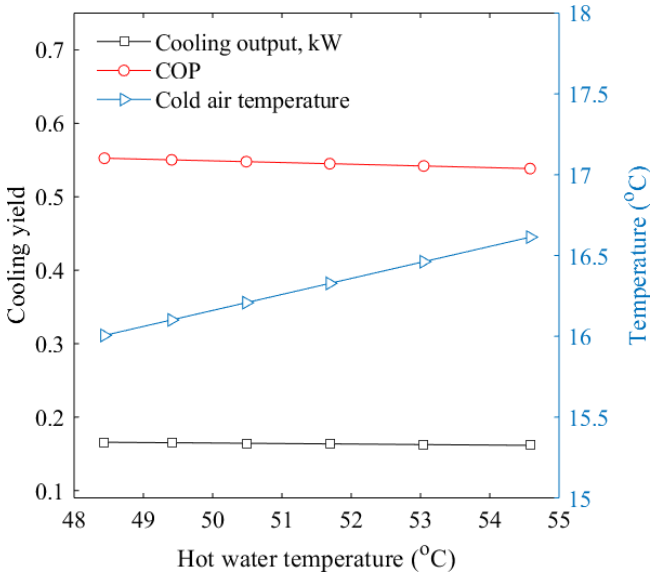

Fig. 10. Role of hot water temperature on cooling yield and cold air temperature of CPVT driven plant at 15 °C chilled water temperature to 3rd dehumidifier.

Results show that increase in hot water temperature results in increased specific water production in both stages of CPVT operated plant. The highest specific water production of 0.12 kg/m^2-h is reached when hot water temperature is around 54.70 °C. At the same time the highest specific water production from the solar flat plat collectors operated plant is 0.11 kg/m^2-h. From the results for the same hot water temperature of 54.70 °C the specific water production from the CPVT operated plant is 8.3% greater than the specific water production of SFPC assisted plant. This is due to

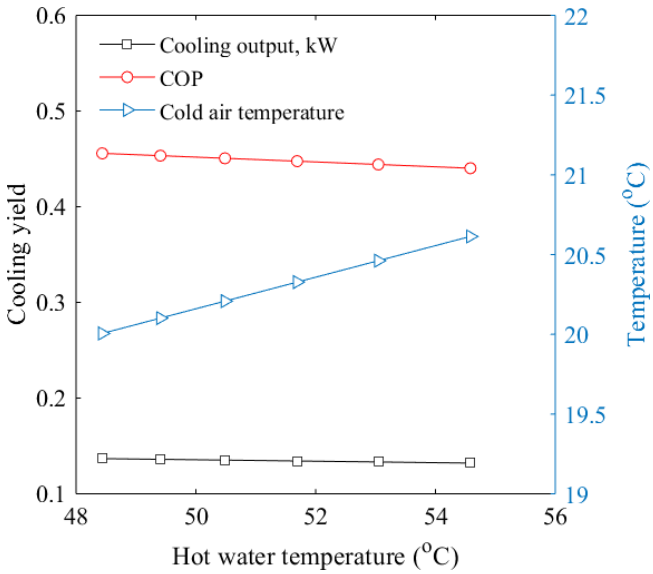

Fig. 11. Role of hot water temperature on cooling yield and cold air temperature of CPVT driven plant at 20 °C chilled water temperature to 3rd dehumidifier.

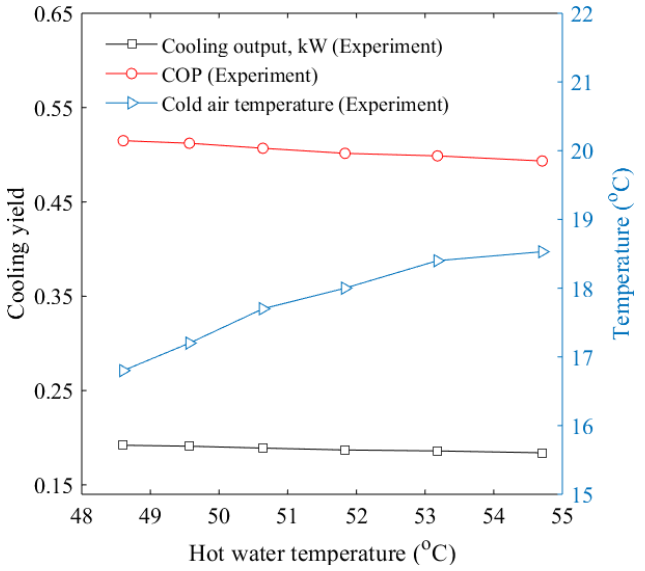

Fig. 12. Role of hot water temperature on cooling yield and cold air temperature of SFPC driven plant at 15 °C chilled water temperature to 3rd dehumidifier.

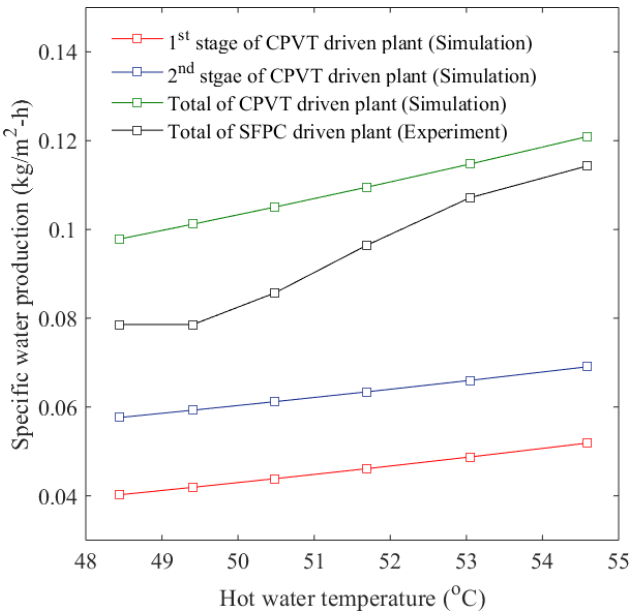

Fig. 13. Role of hot water temperature on specific water production at 15 °C chilled water supply to 3rd dehumidifier.

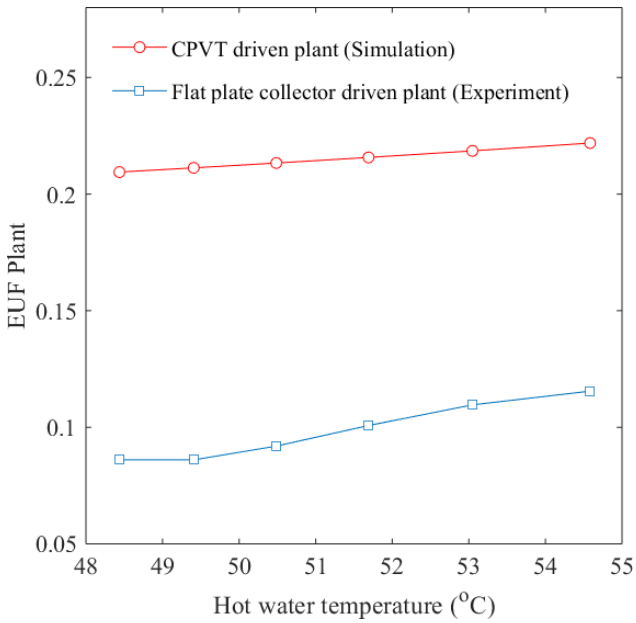

Fig. 14. Role of hot water temperature on plant EUF at 15 °C chilled water supply to 3rd dehumidifier.

that the CPVT system requires less area than the flat plate collectors to produces the same amount of thermal energy required for the combined two stage desalination and cooling system.

Fig. 14 depicts the role of hot water temperature on EUF of plant. The comparative result shows that in both plants, EUF increases as the temperature of hot water increases. This is due to desalination output is relatively high at higher hot water temperature. Meanwhile, cooling output decreases with increase in hot water temperature. Since, the EUF of plant is calculated by Eq. (14), it also depends on net electricity consumption. It is observed that EUF of SFPC driven plant is significantly lesser as it consumes high electrical energy compared to CPVT driven plant. Thus EUF of SFPC assisted plant highly depends on hot water temperature as the plant produces two outputs such as pure water and cooling. But the EUF of CPVT driven plant depends on both hot water temperature as well as electrical power as it produces electricity along with pure water and cooling. The highest EUF for SFPC assisted plant and CPVT collector assisted plants are 0.11 and 0.23 respectively at 54.70 °C of hot water temperature.

5. Conclusions

A performance and comparative analysis of combined desalination and cooling plant was carried out with two different solar collectors as the energy source. The potential and advantage of CPVT collector against solar flat plate collector to operate the TSDC plant for same output was investigated. Effects of hot saline water temperature on desalination yield, cooling output are studied. Both configurations are compared in terms of specific water production and plant EUF. Results show that by using CPVT solar collector for combined desalination and cooling plant, electricity consumption is reduced by 76% while simultaneously supplying required thermal energy. At 54.70 °C of hot saline water temperature, the specific water production and energy utilization factor of CPVT assisted plant are 8.3% and 52.1% higher than the SFPC assisted plant. The CPVT collector assisted desalination and cooling plant has significantly higher specific water production and energy utilisation factor than SFPC assisted plant. Hence CPVT collector is well suitable for the TSDC plant. The study recommends that with proper sizing, the CPVT collector would be a felicitous technologies for standalone cogeneration or trigeneration systems.

Symbols

A — Area, m^2
C_p — Specific heat, kj/kg-K
h — Specific enthalpy, kJ/kg
h_b — Back side convective heat transfer coefficient, W/m^2K
h_f — Front side convective heat transfer coefficient, W/m^2K
I_{bm} — Beam radiation, W/m^2
l — Thickness, m
m — Mass flow rate, kg/s
η — Efficiency
P — Electrical power, kW
Q — Thermal power, kW
T — Temperature, °C
w — Specific humidity, kg/kg dry air

Suffix

a — Ambient
ap — Aperture
APH — Air preheater
b — Back
br — Brine
bw — Brackish water
c — Cell
cw — Circulating water
dw — Distilled water
e — Electrical
f — Front
inv — Inverter
opt — Optical
pl — Plate
pv — Photovoltaic
ref — Refrigerant
s — Saturation
w — Water

Acronyms and abbreviations

CPVT — Concentrated photovoltaic/thermal
PVT — Photovoltaic/thermal
EUF — Energy utilization factor
PVT — Photovoltaic thermal
SFPC — Solar flat plate collectors
SS — Stainless steel
SWP — Specific water production

Acknowledgement

This study is supported by a project grant from the Council of Scientific and Industrial Research (CSIR), New Delhi, India (22(0627)/13/EMR-II).

References

[1] M.A. Antar, M.H. Sharqawy, Experimental investigation on the performance of an air heated humidification-dehumidification desalination system, Desal. Water Treat., 51 (2013) 837–843.
[2] Y. Ghalavand, M.S. Hatamipour, A. Rahimi, A review on energy consumption of desalination process, Desal. Water Treat., (2014) 1–16.
[3] G.P. Narayan, M.H. Sharqawy, E.K. Summers, J.H. Lienhard, S.M. Zubair, M.A. Antar, The potential of solar-driven humidification-dehumidification desalination for small scale decentralized water production, Renew. Sustain. Energy Rev., 14 (2010) 1187–1201.
[4] A.S. Nafey, H.E.S. Fath, S.O. El-Helaby, A. Soliman, Solar desalination using humidification-dehumidification process. Part II. An experimental investigation, Energy Convers. Manag., 45 (2004) 1263–1277.
[5] X. Li, G. Yuan, Z. Wang, H. Li, Z. Xu, Experimental study on a humidification and dehumidification desalination system of solar air heater with evacuated tubes, Desalination, 351 (2014) 1–8.
[6] F.A. Al-Sulaiman, M.I. Zubair, M. Atif, P. Gandhidasan, S.A. Al-Dini, M.A. Antar, Humidification dehumidification desalination system using parabolic trough solar air collector, Appl. Therm. Eng., 75 (2015) 809–816.
[7] T. Rajaseenivasan, K. Srithar, Potential of a dual purpose solar collector on humidification dehumidification desalination, Desalination, 404 (2017) 35–40.
[8] M.A. Younis, M.A. Darwish, F. Juwayhel, Experimental and theoretical of a humidification-dehumidification desalination system, Desalination, 94 (1993) 11–24.
[9] A. Fouda, S.A. Nada, H.F. Elattar, An integrated A/C and HDH water desalination system assisted by solar energy: Transient analysis and economical study, Appl. Therm. Eng., 108 (2016) 1320–1335.
[10] H.F. Elattar, A. Fouda, S.A. Nada, Performance investigation of a novel solar hybrid air conditioning and humidification-dehumidification water desalination system, Desalination, 382 (2016) 28–42.
[11] M. Sadeghi, M. Yari, S.M.S. Mahmoudi, M. Jafari, Thermodynamic analysis and optimization of a novel combined ejector refrigeration cycle-Desalination system, Appl. Energ., 208 (2017) 239–251.
[12] S.A. Nada, H.F. Elattar, A. Fouda, Experimental study for hybrid humidification-dehumidification water desalination and air conditioning system, Desalination, 363 (2015) 112–125.
[13] S. Anand, A. Gupta, S.K. Tyagi, Simulation studies of refrigeration cycles: A review, Renew. Sustain. Energy Rev., 17 (2013) 260–277.
[14] M. Saouliotis, N. Arnaoutakis, G. Panaras, A. Kavga, S. Papaefthimiou, Experimental study and life cycle assessment (LCA) of hybrid photovoltaic/thermal (PV/T) solar systems for domestic applications, Renew. Energ., 126 (2018) 708–723.

[15] P. Ponraj, D.P. Winston, A.E. Kabeel, B.P. Kumar, A.M. Manokar, R. Sathyamurthy, S.C. Christabel, Experimental investigation on Peltier based hybrid PV/T active solar still for enhancing the overall performance, Energy Convers. Manag., 168 (2018) 371–381.
[16] A.M. Manokar, D.P. Winston, A.E. Kabeel, S.A. El-Agouz, R. Sathyamurthy, T. Arunkumar, B. Madhu, A. Ahsan, Integrated PV/T solar still-A mini-review, Desalination, 435 (2018) 259–267.
[17] A. Giwa, H. Fath, S.W. Hasan, Humidification-dehumidification desalination process driven by photovoltaic thermal energy recovery (PV-HDH) for small-scale sustainable water and power production, Desalination, 377 (2016) 163–171.
[18] F. Calise, M.D. d'Accadia, A. Piacentiono, A novel solar trigeneration system integrating PVT (photovoltaic thermal collectors) and SW (seawater) desalination: Dynamic simulation and economic assessment, Energy, (2014) 1–20.
[19] B. Su, W. Qu, W. Han, H. Jin, Feasibility of a hybrid photovoltaic/thermal and liquid desiccant system for deep dehumidification, Energy Convers. Manag., 163 (2018) 457–467.
[20] A. Ramos, M.A. Chatzopoulou, I. Guarracino, J. Freeman, C.N. Markides, Hybrid photovoltaic-thermal solar systems for combined heating, cooling and power provision in the urban environment, Energy Convers. Manag., 150 (2017) 838–850.
[21] C. Renno, F. Petito, Design and modelling of a concentrating photovoltaic thermal (CPV/T) system for a domestic application, Energ. Buildings, 62 (2013) 392–402.
[22] G. Mittelman, A. Kribus, A. Dayan, Solar cooling with concentration photovoltaic/thermal (CPVT) system, Energy Convers. Manag., 48 (2007) 2481–2490.
[23] F. Almonacid, P.J. Perez-Higueras, E.F. Fernandez, P. Rodrige, Relation between the cell temperature of a HCPV module and atmospheric parameters, Sol. Energy Mater Sol. Cells, 105 (2012) 322–327.
[24] A. Kribus, D. Kaftori, G. Mittelman, A. Hirshfeld, Y. Flitsanov, A. Dayan, A miniature concentrating photovoltaic and thermal system, Energy Convers. Manag., 47 (2006) 3582–3590.
[25] C. Chiranjeevi, T. Srinivas, Augmented desalination with cooling integration, Int. J. Refrig., 80 (2017) 106–119.
[26] G.F. Hewitt, G.L. Shires, T.R. Bott, Process Heat Transfer, CRC Press, NewYork, Begell House,1994.
[27] W.F. Stoecker, J.W. Jones, Refrigeration and Air Conditioning, McGraw-Hill, New York, 1982.
[28] K. Nishioka, T. Takamoto, T. Agui, M. Kaneiwa, Y. Uraoka, T. Fuyuki, Annual output estimation of concentrator photovoltaic system using high-efficiency InGaP/InGaAs/Ge triple-junction solar cells based on experimental solar cell's characteristics and field-test metrological data, Sol. Energy Mater Sol. Cells, 90 (2006) 57–67.